

Preliminary Development of a Comprehensive Calibrated Subsurface Pathway Simulator for the Subsurface Disposal Area at the Idaho National Engineering and Environmental Laboratory

Swen Magnuson, Jeff Sondrup, and Bruce Becker
 Lockheed Martin Idaho Technologies Company
 Idaho National Engineering and Environmental Laboratory

ABSTRACT

The first detailed comprehensive simulation study to evaluate fate and transport of low-level, mixed, and transuranic wastes buried in the Subsurface Disposal Area (SDA) at the Idaho National Engineering and Environmental Laboratory (INTEL) has recently been conducted. The study took advantage of pertinent information relating to describing aqueous- and vapor-phase movement of contaminants in the primarily fractured basalt subsurface. The study included spatially and temporally variable infiltration, barometric pressure changes, positive down-hole air pressure during well drilling, vapor-vacuum extraction, and regional hydraulic gradients. Use of the TETRAD simulation code allowed all the pertinent information to be included into a single comprehensive model of the SDA subsurface. An overview of the model implementation and comparisons of calibrated model results to the observed vadose zone water distribution, volatile organic vapor concentrations, and aqueous concentrations of volatile organics and nitrate are presented. Additionally, comparisons between simulated and observed concentrations for other contaminants which were not used for model calibration are made.

As part of this modeling exercise, inadequacies in the available data relating to characterization of non-sorbing aqueous-phase transport have been identified. Even with the identified data inadequacies, the comparisons between simulated and observed contaminants along with the calibration results give confidence that the model is a conservative representation of flow and transport in the subsurface at the SDA. The results from this modeling study are being used to guide additional data collection activities at the SDA for purposes of increasing confidence in the appropriateness of model predictions.

This work was funded by the U.S. Department of Energy under DOE Idaho Operations Office Contract DE-AC07-94ID13223.

INTRODUCTION AND BACKGROUND

The SDA is part of the Radioactive Waste Management Complex located in the southwest portion of the INTEL. Low-level, mixed, and transuranic radioactive wastes were buried in shallow pits and trenches in the SDA from 1952 until 1970. Since 1970, transuranic waste has been stored in above-grade facilities. Mixed-waste disposal ceased in 1982. Currently, low-level waste is still being disposed in a portion of the SDA. The SDA overlies a thick stratigraphic sequence composed primarily of fractured basalts that are occasionally interrupted by sedimentary interbeds that were deposited during extended periods of volcanic quiescence. The basalt flows are named alphabetically corresponding to the stratigraphic sequence with the youngest flow being called "A". The interbeds are named based on the basalt flows that overlie and underlie them. The three primary sedimentary interbeds beneath the SDA are called the A-B, B-C, and C-D interbeds and occur at depths of approximately 10, 30, and 70 m below land surface. Both the upper surface and thickness of the interbeds vary spatially. In the SDA vicinity, the A-B interbed thickness ranges from 0 to 3.4 m and, where it is present, averages 1.6 m. The B-C interbed thickness ranges from 0 to 12 m and averages 3.4 m. The C-D interbed thickness ranges from 0 to 10.7 m and averages 4.4 m. There are deeper interbeds beneath the SDA but the limited wellbore information indicates they are much less continuous.

DISTRIBUTION OF THIS DOCUMENT IS UNLIMITED

MASTER

Un

DISCLAIMER

This report was prepared as an account of work sponsored by an agency of the United States Government. Neither the United States Government nor any agency thereof, nor any of their employees, makes any warranty, express or implied, or assumes any legal liability or responsibility for the accuracy, completeness, or usefulness of any information, apparatus, product, or process disclosed, or represents that its use would not infringe privately owned rights. Reference herein to any specific commercial product, process, or service by trade name, trademark, manufacturer, or otherwise does not necessarily constitute or imply its endorsement, recommendation, or favoring by the United States Government or any agency thereof. The views and opinions of authors expressed herein do not necessarily state or reflect those of the United States Government or any agency thereof.

DISCLAIMER

Portions of this document may be illegible electronic image products. Images are produced from the best available original document.

The Snake River Plain Aquifer (SRPA) underlies the SDA beginning at a depth of approximately 175 m below land surface.

The primary purpose of the SDA simulation study was to perform fate and transport calculations to support an Interim Risk Assessment (IRA) being conducted for the Waste Area Group (WAG) 7 Operable Unit (OU) 7-13/14 comprehensive remedial investigation/feasibility study (RI/FS). The overall approach was to develop a simulation model representative of flow and transport in the subsurface. Representativeness was obtained and demonstrated by calibrating model results to observed water and contaminant data and is a substantial improvement over earlier simulation studies. A secondary purpose of the SDA simulation study was to be able to use the model to evaluate possible remediation strategies and their effects on flow and transport in the OU 7-13/14 feasibility study.

CONCEPTUAL MODEL

The conceptual model used for the flow simulation consisted of spatially variable and time-dependent infiltration at the surface of the SDA. Infiltrating water moved downward under the influence of gravity and capillarity. Downward movement occurred within both the fractured basalt flows and sedimentary interbeds that compose the vadose zone beneath the SDA. The sedimentary interbeds had both variable thickness and variable elevations to the overlying and underlying basalt flow contacts. Perched or near-perched water conditions occurred in association with the sedimentary interbeds when adequate water was either supplied from above or through horizontal movement within the vadose zone. Water movement within the fractured basalts was considered to be controlled primarily by the fracture network. Water that infiltrated at the surface eventually reached the SRPA. Horizontal movement of water within the SRPA caused the water that originally infiltrated at the SDA surface to move laterally within the aquifer.

The transport conceptual model assumed contaminant movement is controlled primarily by advection and dispersion. Because the flow conceptual model consisted of water movement primarily within the higher permeability fractures and rubble zones in the basalt portions of the subsurface, sorption of contaminants onto surfaces within the basalt matrix was considered not to occur. Rather, sorption occurred onto fine-grained sediments or chemical and weather alteration products coating the surfaces of the fractures through which water and contaminants moved. Sorption onto these fracture coatings was estimated based on assumed effective fracture geometries. Including sorption in this manner implied that the basalt matrix did not effect dissolved-phase transport. This is consistent with the simulation results (Magnuson 1995) from the Large Scale Aquifer Pumping and Infiltration Test conducted near the SDA (Wood and Norrell, 1996). Updated estimates of the sediment sorption properties for each contaminant were used. Diffusion of contaminants within the aqueous phase in the fracture system was considered. Diffusion of aqueous phase contaminants into the basalt matrix was neglected. As appropriate, radioactive decay and ingrowth also were included.

The transport conceptual model was further expanded to account for contaminants such as volatile organic compounds (VOCs) that migrate in both the dissolved and vapor phase. This expanded model used the dissolved phase transport conceptual model and further included vapor phase advection, dispersion, and diffusion in a dual porosity system. Partitioning of the VOCs between the aqueous and vapor phases was included. Tortuosity of the porous media was used to modify the mobility of the volatile contaminants in the vapor phase. Influences from barometric pressure fluctuations, air injection from drilling of ~40 wells by air-rotary methods, past vapor extraction events, and buoyancy effects also were included. Release of VOCs to the atmosphere was by both advection and diffusion in the vapor phase. The source term release conceptual model, development and implementation for this SDA simulation study is presented in a separate companion paper.

SIMULATION CODE

The TETRAD code (Vinsome and Shook 1993) was chosen to simulate flow and transport. TETRAD has complete multi-phase, multi-component simulation capabilities. Movement of any number of components within aqueous, gaseous, and oleic phases were considered in the SDA simulation study. TETRAD uses a block-centered finite-difference approach and has capabilities for local grid refinement, which were used extensively. The TETRAD simulator also includes dual porosity simulation capabilities. This feature was used to address gaseous-phase movement in both the fracture and matrix portions of the fractured basalts comprising the majority of the subsurface beneath the SDA.

FLOW MODEL

Stratigraphic information on ~90 wells in the SDA vicinity from a United States Geological Survey database were used to assign lithologic properties to the three-dimensional simulation domain. A base grid encompassing the region from north of the SDA to the southern INEEL boundary was defined. Three levels of grid refinement were used in the vicinity of the SDA to provide increased numerical resolution. This refinement was done both vertically and horizontally. Kriging using detrended lithologic data was used to define the depths of the surficial sediments, and the upper surfaces and thickness of the three primary interbeds in the SDA subsurface: the A-B, B-C, and C-D interbeds. These interpreted surfaces were then used to define material property boundaries in the discretized model (Figure 1). Where the discretization was not fine enough to preserve known gaps or "holes" in the interbeds, gaps were manually superimposed onto the kriging results.

Hydrologic property estimates came from sediment sample analyses (Magnuson and McElroy 1993), basalt matrix characterization (Bishop 1991), and inverse modeling (Magnuson 1995) of the Large Scale Aquifer Pumping and Infiltration Test for the basalt fracture network.

Surface boundary conditions consisted of spatially-varying infiltration (Figure 5). The results of neutron access-tube monitoring at twenty locations inside the SDA was used to develop transient descriptions of infiltration at each monitoring location (Martian, 1995). Three of these locations were selected as representative of low, medium, and high infiltration rates. The time-averaged equivalent infiltration rates were 1, 4, and 24 cm/year for the low, medium, and high regions, respectively. If these three rates are averaged according to their spatial distribution across the SDA, the overall average infiltration rate is 8.5 cm/year.

Three historical flooding events at the SDA (1962, 1969, and 1982) were included in the simulation. Estimates of the volume of additional water that infiltrated were based on work by Vigil (1988). The transient descriptions of infiltration resulted in pulses of water that infiltrated but were damped out with increasing depth as successive interbeds were encountered.

Measured SRPA water levels from 1994 were used to assign prescribed head boundaries on the sides of the saturated portion of the simulation domain. Three permeability regions were assigned to achieve adequate agreement between simulated and measured aquifer water levels.

Calibration objectives in the vadose zone were the spatial occurrence and temporal behavior of perched water that occurs in association with the interbeds. The perched water behavior in the surficial sediments was not used since it was part of the infiltration model calibration. Although the final calibrated results from the flow model were judged to be adequate for simulating fate and transport, the level of discretization in the deeper interbeds was not adequate to allow detailed modeling of perched water behavior.

Primary changes to parameters made as part of the flow calibration were:

- Reduced anisotropy of fractured basalt domain from 300:1 to 30:1.
- Reduced permeability of upper grid blocks in B-C and C-D interbeds to emulate low-permeability clay.

Primary observations from the flow modeling were:

- Perched water occurred more frequently and with greater lateral extent in the transient infiltration simulation.
- Water movement in the simulations was complex. Lateral movement of water and saturation within the interbeds varied both spatially and temporally.
- Both the B-C and C-D interbeds were generally wetter to the south, primarily because of a south-southeast general down-dip direction in both interbeds.

DISSOLVED-PHASE TRANSPORT MODEL

Fifty two contaminants were identified for modeling as part of the IRA. From these contaminants, nitrate was selected as the best candidate for calibration of the dissolved-phase transport model. Based on the aquifer monitoring results, there was the possibility of a contribution to nitrate concentrations within the SRPA from the SDA (Figure 3) that could be used for calibration of the dissolved-phase transport model. This determination was complicated by the presence of nitrate in the aquifer from upgradient (relative to flow within the SRPA) sources. An estimate of the SDA local background concentration of 700 $\mu\text{g-N/L}$ was made by Burgess (1996). This local background concentration was assumed to be correct and the portion of the nitrate concentrations above this level were assumed to come from the SDA for purposes of model calibration. This was a conservative assumption since it implies there is already a contribution from the SDA when it cannot be stated unequivocally that there is such a contribution. There is a markedly small number of samples that have been taken from the vadose zone that could be used for transport calibration for any contaminant and especially for nitrate since nitric acid has been added as a preservative for perched water samples.

The nitrate release estimated from the source term model was spatially distributed across the SDA (Figure 2). Best-estimates of the nitrate inventory disposed of in the SDA were used for the transport calibration. The calibrated flow model was used and dispersivities were adjusted in the aquifer to improve the agreement between measured and simulated results. Figure 2 also shows a comparison of measured and simulated results for one well as an example.

Primary observations from the dissolved-phase transport modeling were:

- The model predicted nitrate concentrations to be increasing in the aquifer.
- The effect of gaps in the B-C interbed influenced early (pre-1970) concentrations at depth in the aquifer.
- The south-southeast dip in the B-C and C-D interbeds shifted the location of highest concentration in the aquifer to the south and east with increasing time.

- The transport model did a reasonable job of emulating the portion of the nitrate concentrations that were assumed to be from wastes buried in the SDA.

COMBINED AQUEOUS- AND GASEOUS-PHASE TRANSPORT MODEL

The calibrated dissolved-phase transport model was further used to calibrate a transport model for VOCs. VOC source locations (Figure 2) were based on historic disposal data, soil gas survey information, and model calibration results. Carbon tetrachloride (CCl_4) was chosen to calibrate the VOC transport model because the disposal history was thought to be relatively well known and it is prevalent in the vadose zone and groundwater. Carbon tetrachloride release was governed by the inventory, drum failure rate, and diffusion from a sludge waste form.

The following parameters and conditions were investigated during the CCl_4 calibration process: drum failure rate, diffusivity from the sludge, source inventory, source location, vapor phase tortuosities, possible existence of an extensive high permeability layer (rubble zone), basalt matrix porosity, and the amount of air injected during well drilling.

Calibration simulation results were compared to averaged vertical vapor concentration profiles at specific wells, and time histories of vapor concentrations at specific ports, and time histories of groundwater concentrations at specific wells. Figure 4 shows comparisons for two vadose zone vapor monitoring ports and for two aquifer monitoring wells. Comparisons also were made to surface flux and perched water data, but lesser emphasis was given to these comparisons because of the minimal data set.

Primary observations from the CCl_4 modeling were:

- The final calibrated model showed agreement in magnitude and trend of CCl_4 measurements in the vadose zone and in the aquifer. This agreement was best in the high concentration areas at depth beneath the center of the SDA. Grid resolution was inadequate for making comparisons to near surface vapor concentrations.
- The model predicted that of the CCl_4 released from disposal locations, ~80% has been released to the atmosphere, ~20% is in the vadose zone, and <1% has gone into the aquifer.
- The estimated CCl_4 inventory had to be increased to match the observed vadose zone vapor concentrations and aquifer concentrations.

PREDICTIVE MODELING

Using the calibrated flow and transport models, 52 contaminants that remained after a screening process were simulated using upper bound inventory estimates as required by CERCLA. These predicted concentrations were then used in the risk calculations for the IRA. Eight contaminants (carbon tetrachloride, methylene chloride, tetrachloroethene, tritium, chlorine-36, butanone, acetone, and hydrazine) were simulated with the combined aqueous and vapor-phase model. Table I contains comparisons of maximum observed concentrations of each of these contaminants to maximum simulated concentrations anywhere in the model at a depth equivalent to the monitoring locations. It is important to keep in mind when making these comparisons that upper bound inventories were used for the predictive simulations and that the location of maximum concentration in the simulation does not correspond to any of the available aquifer monitoring locations.

SENSITIVITY AND UNCERTAINTY

The sensitivity of contaminants to selected hydrologic and transport parameters was qualitatively determined during the flow and transport calibration process, which resulted in the following observations:

- The nitrate calibration is uncertain because of limited data that do not clearly indicate a contribution from the SDA to observed aquifer concentrations. By assuming an SDA contribution above the local estimated background, the model was conservative because the contaminants were modeled to have already reached the aquifer by dissolved-phase transport.
- The modeled aquifer concentrations were relatively insensitive to longitudinal dispersivity in general; however, they were somewhat sensitive to transverse dispersion.
- For CCl_4 transport, the sensitivity to boundary condition influences was most pronounced for atmospheric pressure fluctuations at land surface, positive pressure air injection during well drilling, and vapor vacuum extraction activities.
- The transport of CCl_4 was sensitive to diffusion, which is controlled by tortuosity. The uncertainty associated with tortuosity was large.
- The transport of CCl_4 was highly sensitive to the source release rate, which is a combined function of the CCl_4 inventory, drum failure rate, and diffusivity from the sludge waste form.
- Though the sensitivity to hydrologic parameters generally was slight, the dissolved-phase concentrations were generally found to be much more sensitive to the inventory and simulated source release mechanisms than any of the hydrologic parameters in the subsurface transport model.

Given the results of the qualitative sensitivity analysis, the largest uncertainties in the predictive simulation results were from uncertainties related to the source term inventory and the description of release mechanisms from buried waste. Uncertainties from the hydraulic and transport parameters used in modeling were smaller than those associated with inventory with the possible exception of some of the partition coefficients that were used.

CONCLUSIONS

This simulation study represents the first attempt to make an all-inclusive effort to simulate contaminant transport of wastes buried in the SDA. Lack of sufficient data from the vadose zone beneath the SDA limit the ability to completely calibrate a transport model. Although there is considerably more aquifer data available, no clear contribution from the SDA can be discerned because of contamination from upgradient facilities.

The process of performing this SDA simulation study has in part been responsible for the initiation of the following additional or continued characterization activities:

- Sampling will continue in available vadose zone locations utilizing existing suction lysimeters and perched water wells. Sample results in the vadose zone are beneficial for model calibration (and thus risk assessment) since they are closer to the source release area and are not subject to interpretation complications from upgradient sources relative to flow in the SRPA.

- Four new upgradient aquifer monitoring wells have been proposed to allow determination of possible contribution from SDA waste migration to aquifer concentrations.
- Drilling through waste pits has been proposed to collect samples for determination of contaminant geochemical form and mobility.
- Suction lysimeters and moisture monitoring instruments are proposed to be placed in the pit characterization drill holes to allow monitoring of concentrations in leachate and determination of the amount of water infiltrating through the waste. Sampling of leachate directly beneath the disposal locations would benefit the source release modeling due to uncertainties in inventory and release mechanisms.

Results from these additional activities will be useful in either validating the results of this simulation study or guiding future studies.

REFERENCES

1. J.D. BURGESS, "Tritium and Nitrate Concentrations at the RWMC," INEL-96/204, Idaho National Engineering and Environmental Laboratory (1996).
2. C.W. BISHOP, "Hydraulic Properties of Vesicular Basalt," Masters Thesis, University of Arizona (1991).
3. S.O. MAGNUSON and D.L. MCELROY, 1993, "Estimation of Infiltration from In Situ Moisture Contents and Representative Moisture Characteristic Curves for the 30', 110', and 240' Interbeds," Engineering Design File RWM-93-001.1, Idaho National Engineering and Environmental Laboratory (1993).
4. S.O. MAGNUSON, "Inverse Modeling for Field-Scale Hydrologic and Transport Parameters of Fractured Basalt," INEL-95/0637, Idaho National Engineering and Environmental Laboratory (1995).
5. P. MARTIAN, "UNSAT-H Infiltration Model Calibration at the Subsurface Disposal Area, Idaho National Engineering Laboratory," INEL-95/0596, Idaho National Engineering and Environmental Laboratory (1995).
6. M.J. VIGIL, 1988, "Estimate of Water in Pits During Flooding Events," Engineering Design File BWP-12, Idaho National Engineering and Environmental Laboratory (1988).
7. P.K.W. VINSOME and G.M. SHOOK, "Multi-Purpose Simulation," Journal of Petroleum Science and Engineering, Volume 9, pp. 29-38 (1993).
8. T.R. WOOD and G.T. NORELL, "Integrated Large-Scale Aquifer Pumping and Infiltration Tests, Groundwater Pathways OU 7-06, Summary Report," INEL-96/0256, Rev 0., Idaho National Engineering and Environmental Laboratory (1996).

Table I. Comparison of maximum simulated concentrations through April 1995 to observed COPC concentration measurements since 1987.

COPC	Maximum Simulated Concentration Through 1995 (pCi/L or μ g/L)	Range of Observed Concentrations Above Background in SDA Vicinity Wells Since 1987 (pCi/L or μ g/L)	Number of Wells with Detections	Total Number of Detections Above Background	Comments
Ac ²²⁷	6×10^{-8}	-	-	-	-
Am ²⁴¹	1×10^{-6}	0.04 to 0.3	6	7	Model results agreed with nondetects (NDs), sampling data were erratic.
Am ²⁴³	2×10^{-11}	-	-	-	-
C ¹⁴	5×10^0	3.3 to 28	3	5	Model overpredicted NDs and agree with 20 results from erratic sampling data.
Cl ³⁶	1×10^0	-	-	-	-
Cm ²⁴⁴	2×10^{-9}	-	-	-	-
Co ⁶⁰	4×10^{-9}	-	-	-	-
Cs ¹³⁷	1×10^{-7}	0 to 1,020	4	5	Model agreed with NDs, sampling data were erratic.
Eu ¹⁵²	1×10^{-10}	-	-	-	-
Eu ¹⁵⁴	2×10^{-8}	-	-	-	-
H ³	2×10^3	700 to 3,550	10	147	Model slightly overpredicted measured concentrations. Predictions are consistent with estimated local background from upgradient sources.
I ¹²⁹	4×10^0	17	1	1	Model slightly overpredicted NDs, sampling data were erratic.
Na ²²	5×10^{-1}	-	-	-	-
Nb ⁹⁴	1×10^{-14}	-	-	-	-
Ni ⁵⁹	3×10^{-7}	-	-	-	-
Ni ⁶³	8×10^{-6}	-	-	-	-
Np ²³⁷	8×10^{-4}	-	-	-	-
Pa ²³¹	1×10^{-6}	-	-	-	-
Pb ²¹⁰	4×10^{-8}	-	-	-	-
Pu ²³⁸	1×10^{-12}	0.05 to 0.07	2	2	Model agreed with NDs, sampling data were erratic.
Pu ²³⁹	2×10^{-11}	-	-	-	-
Pu ²⁴⁰	7×10^{-12}	0.04 to 0.4	4	5	Model agreed with NDs, sampling data were erratic.
Pu ²⁴¹	3×10^{-11}	-	-	-	-
Pu ²⁴²	3×10^{-16}	-	-	-	-
Ra ²²⁶	1×10^{-8}	-	-	-	-
Ra ²²⁸	8×10^{-12}	-	-	-	-
Sr ⁹⁰	5×10^{-3}	1.8 to 6.4	6	12	Model agreed with NDs, sampling data were erratic.
Tc ⁹⁹	5×10^1	0.07 to 7.42	6	13	Model overpredicted NDs and slightly overpredicts presumed false positives associated with 1996 sampling that ranged from 4 to 7 pCi/L

Table I. Comparison of maximum simulated concentrations through April 1995 to observed COPC concentration measurements since 1987 (continued).

COPC	Maximum Simulated Concentration Through 1995 (pCi/L or μ g/L)	Range of Observed Concentrations Above Background in SDA Vicinity Wells Since 1987 (pCi/L or μ g/L)	Number of Wells with Detections	Total Number of Detections Above Background	Comments
Th ²²⁸	2×10^{-5}	-	-	-	-
Th ²²⁹	4×10^{-8}	-	-	-	-
Th ²³⁰	8×10^{-7}	-	-	-	-
Th ²³²	1×10^{-11}	-	-	-	-
U ²³²	6×10^{-5}	-	-	-	-
U ²³³	3×10^{-4}	-	-	-	-
U ²³⁴	5×10^{-2}	-	-	-	-
U ²³⁵	3×10^{-3}	-	-	-	-
U ²³⁶	2×10^{-3}	-	-	-	-
U ²³⁸	4×10^{-2}	-	-	-	-
Antimony	2×10^{-7}	4.0 to 11.2	5	6	Model agreed with NDs, sampling data were erratic.
Beryllium	8×10^{-12}	0.7 to 9.1	8	19	Model agreed with NDs, sampling data were erratic.
Cadmium	2×10^{-8}	2.0 to 26.0	8	35	Model possibly underpredicted sampling data. Sampling data showed ratio of greater than 3 for total detections to wells with detections.
Chromium	1×10^{-1}	2.0 to 99.6	19	95	Model underpredicted by one order of magnitude. Sampling data were consistent.
Nickel	3×10^{-13}	1.0 to 42.5	5	17	Model agreed with NDs, sampling data were erratic.
Nitrate	1.4×10^{-4}	1.2 to 3.5×10^{-3}	11	60	This was a calibration target. Overprediction was expected since upper bound inventory estimates were used for predictive simulations.
Lead	3×10^{-8}	5.0 to 46.1	9	18	Model agreed with NDs, sampling data were erratic.
Mercury	6×10^{-10}	0.11 to 1.1	5	10	Model agreed with NDs, sampling data were erratic.
Butanone	2×10^{-4}	6.0 to 10.0	2	2	Model agreed with NDs, sampling data were erratic.
Acetone	5×10^{-4}	3.0 to 35.0	6	8	Model agreed with NDs, sampling data were erratic.
Hydrazine	4×10^{-4}	-	-	-	-
Carbon tetrachloride	8×10^0	0.4 to 7.0	8	137	This was a calibration target.
Methylene chloride	1×10^{-1}	0.2 to 6.0	7	22	Model slightly underpredicted if the sampling data are to be believed. Sampling data showed detection ratio of ~3.
Tetrachloroethene	6×10^{-1}	0.1 to 0.5	5	15	Model agreed with detections. Sampling data showed detection ratio of 3.

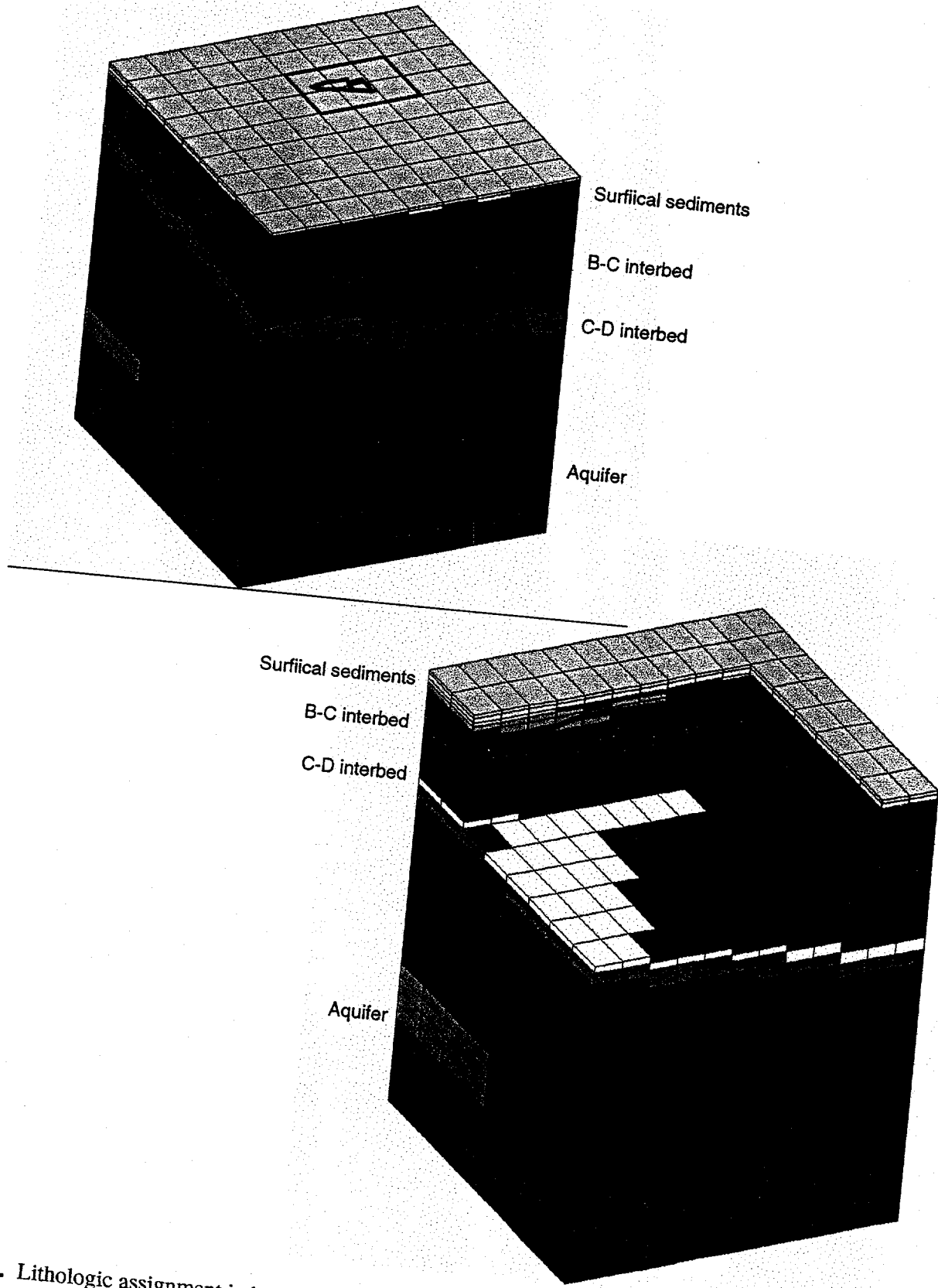


Fig. 1. Lithologic assignment in base and first level of grid refinement with cutaway.

Subsurface Disposal Area

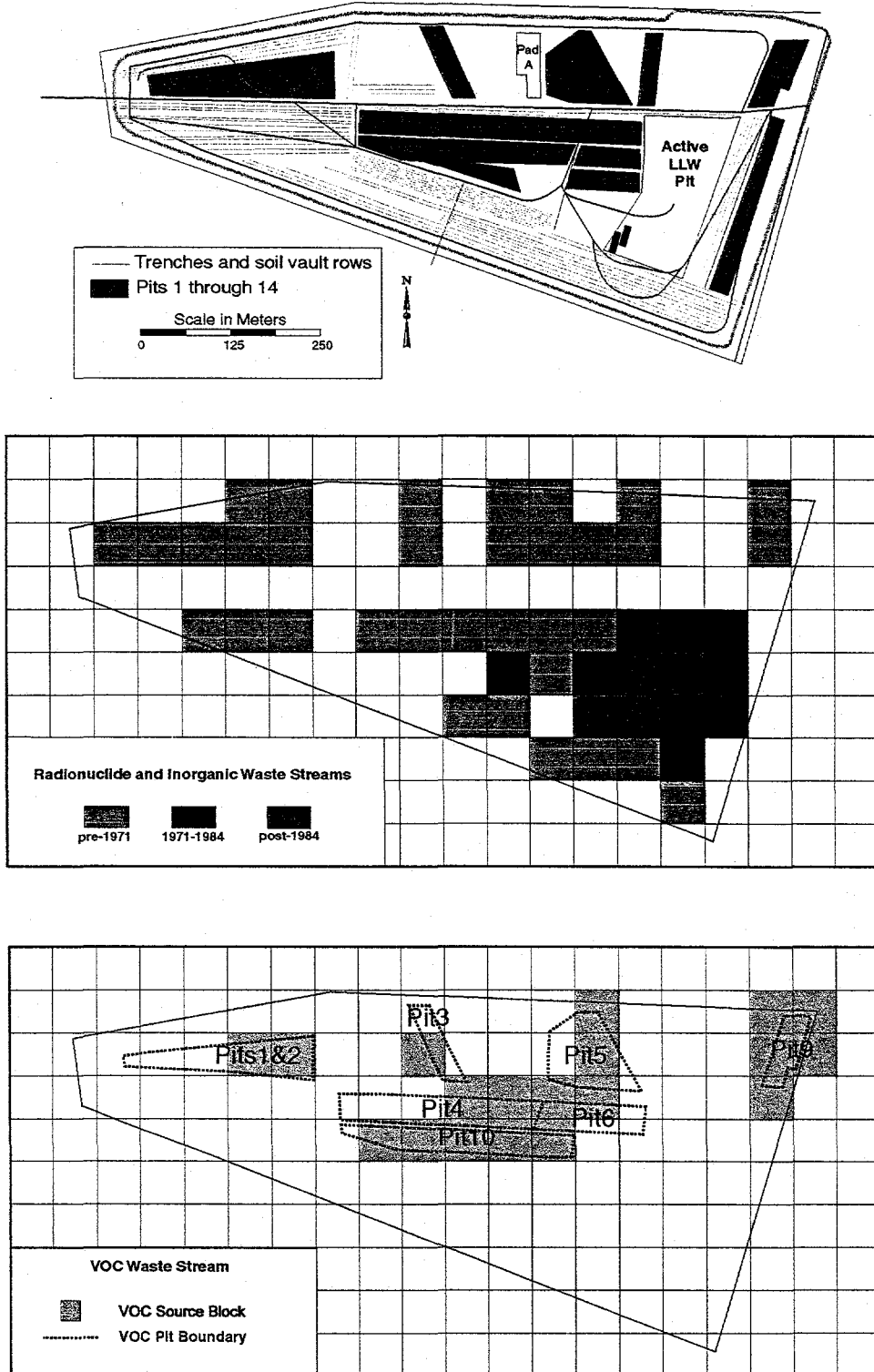


Fig. 2. Subsurface disposal area and assignment of contaminant source releases for simulations.

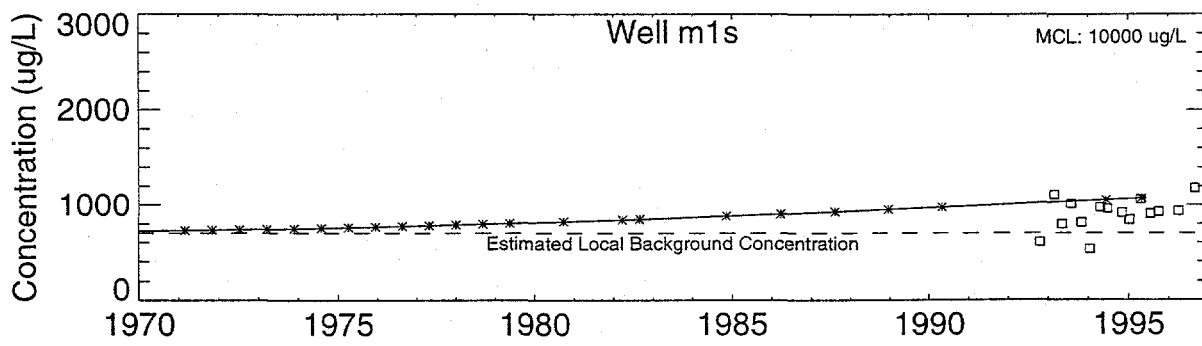
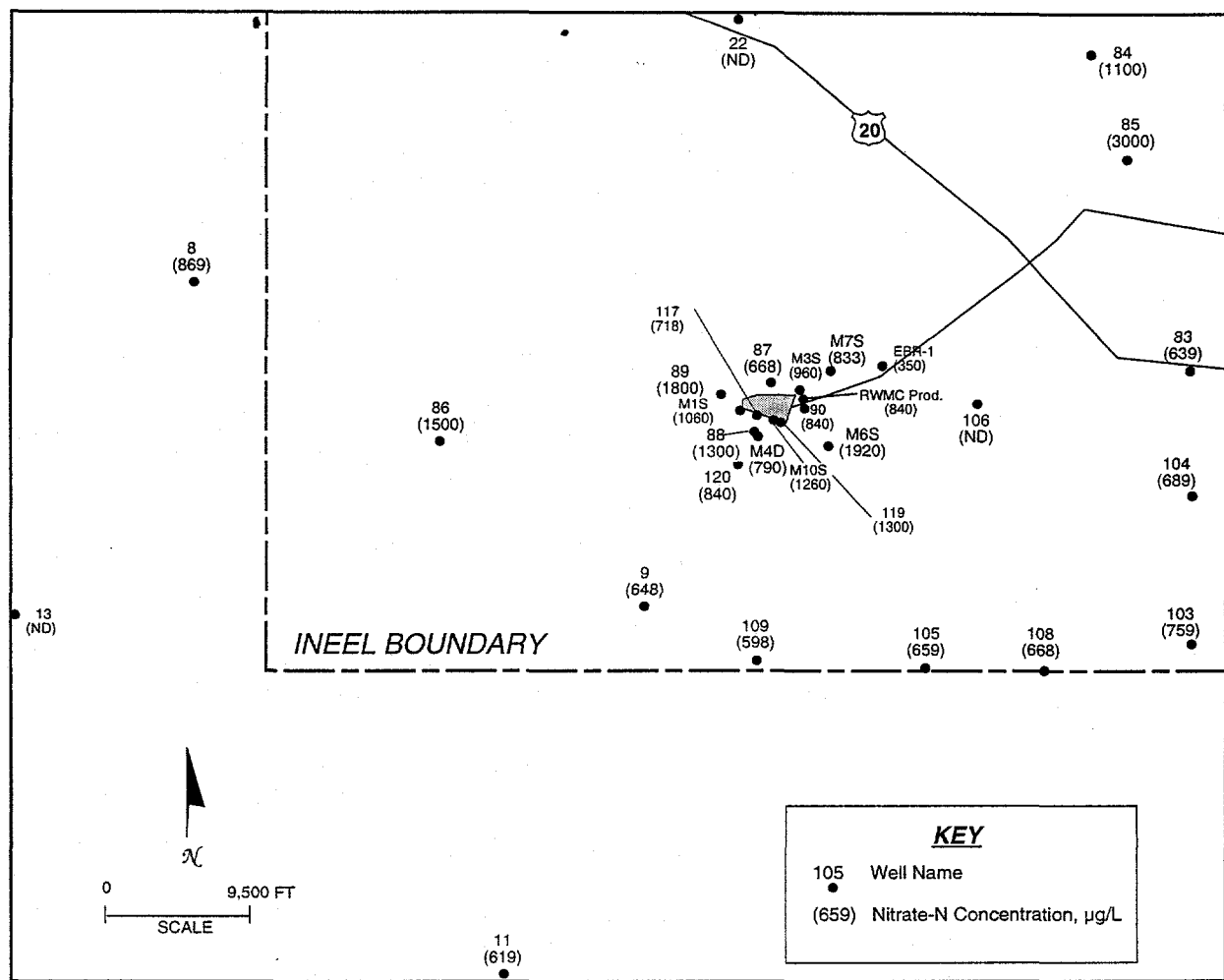


Fig. 3. Distribution of nitrate in groundwater in the southwestern INEEL based on sampling in 1994 and 1995 and simulated (asterisks) and measured (boxes) nitrate aquifer concentrations in one well.

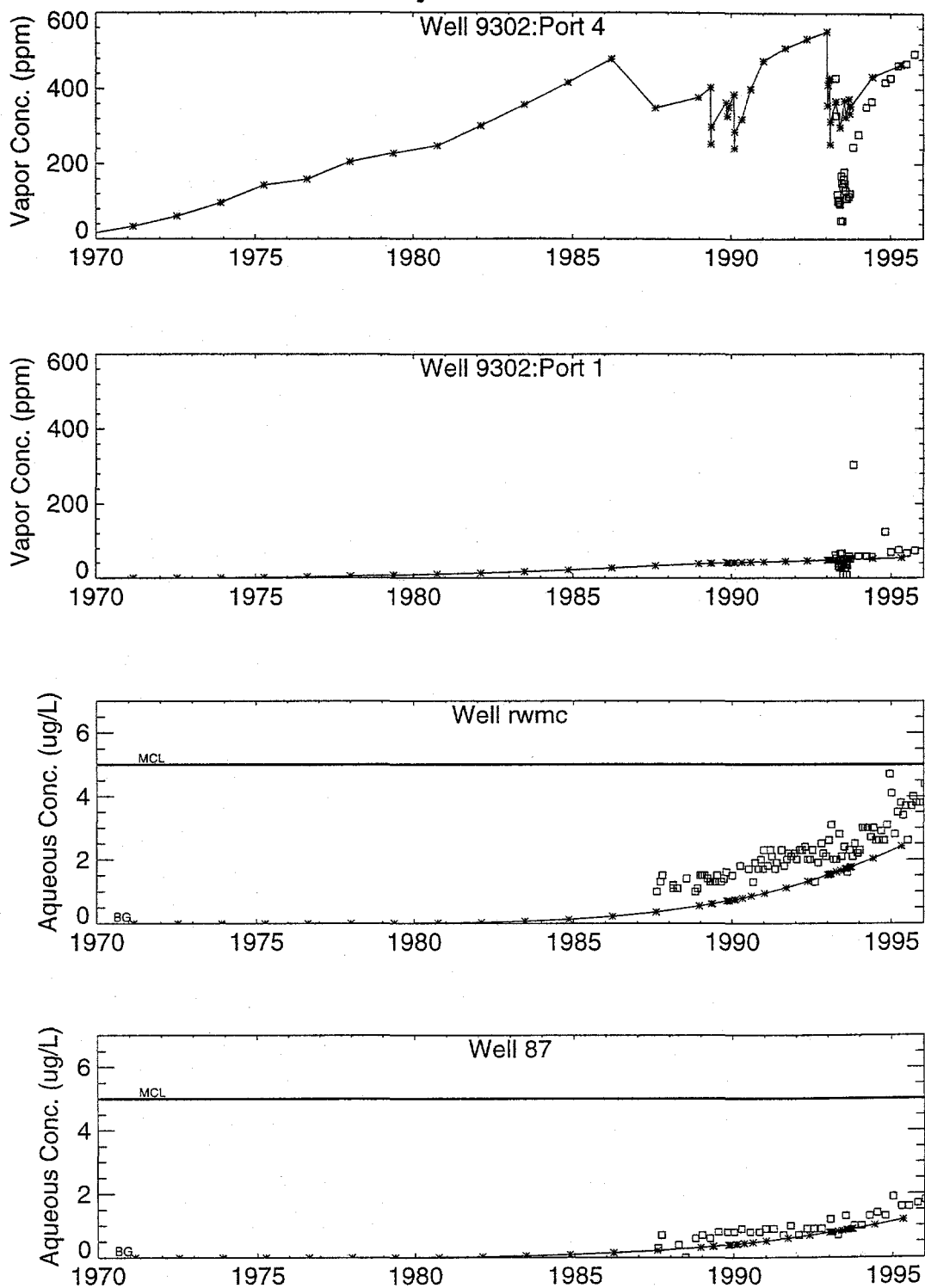


Fig. 4. Simulated (asterisks) and measured (boxes) CCl_4 vadose zone vapor and aquifer concentrations.